Valproic acid Suppresses Breast Cancer Cell Growth Through Triggering Pyruvate Kinase M2 Isoform Mediated Warburg Effect

Zhen Li[1] ⑩, Lina Yang[2], Shuai Zhang[3], Jiaqi Song[4], Huanran Sun[4], Changliang Shan[4], Dan Wang[5], and Shuangping Liu[2]

Abstract

Energy metabolism programming is a hallmark of cancer, and serves as a potent target of cancer therapy. Valproic acid (VPA), a broad Class I histone deacetylases (HDACs) inhibitor, has been used as a therapeutic agent for cancer. However, the detail mechanism about the potential role of VPA on the Warburg effect in breast cancer remains unclear. In this study, we highlight that VPA significantly attenuates the Warburg effect by decreasing the expression of pyruvate kinase M2 isoform (PKM2), leading to inhibited cell proliferation and reduced colony formation in breast cancer MCF-7 and MDA-MB-231 cells. Mechanistically, Warburg effect suppression triggered by VPA was mediated by inactivation of ERK1/2 phosphorylation through reduced HDAC1 expression, resulting in suppressing breast cancer growth. In summary, we uncover a novel mechanism of VPA in regulating the Warburg effect which is essential for developing the effective approach in breast cancer therapy.

Keywords

Warburg effect, Valproic acid, pyruvate kinase M2 isoform, histone deacetylases, cell proliferation, breast cancer

Abbreviations

GEO, Gene Expression Omnibus; ERK1/2, extracellular signal-regulated kinase; HDACs, histone deacetylases; PEP, phosphoenolpyruvate; PK, pyruvate kinase; PKM2, pyruvate kinase M2 isoform; VPA, Valproic acid

Introduction

In 2020, breast cancer is the most commonly occurring cancer all over the world[1]. Breast cancer is one of the most important lethal malignancies threatening women's health worldwide, which is also the leading cause of cancer mortality[1]. Despite remarkable advances have obtained in researches for treating breast cancer, it remains a severe health problem with the abysmal prognosis, due to breast cancer is prone to metastases[2]. Thus, exploring promising strategies to uncover the underlying mechanism of breast cancer development and identifying new targets for breast cancer diagnosis and treatment are essential.

Dr. Otto Warburg demonstrated that cancer cells take more glucose, leading to high rate of robust glycolysis and lactate production even under sufficient oxygen conditions. This phenomenon is widely termed as the Warburg effect, which is a hallmark of cancer[3]. There are growing studies

[1] Biomedical Translational Research Institute, Jinan University, Guangzhou, Guangdong, China
[2] Department of Pathology, Medical School, Dalian University, Dalian, Liaoning, China
[3] School of Integrative Medicine, Tianjin University of Traditional Chinese Medicine, Tianjin, China
[4] State Key Laboratory of Medicinal Chemical Biology, College of Pharmacy and Tianjin Key Laboratory of Molecular Drug Research, Nankai University, Tianjin, China
[5] Department of Pharmacology, Yanbian University, Yanji, Jilin, China

Corresponding Authors:
Shuangping Liu, Department of Pathology, Medical School, Dalian University, Dalian, Liaoning 116622, China.
Email: liushuangping@dlu.edu.cn

Dan Wang, Department of Pharmacology, Yanbian University, Yanji, Jilin 133002, China.
Email: wangdan@ybu.edu.cn

showing that kinds of metabolism enzymes are up-regulated or activated during tumorigenesis and targeting altered energy metabolism is an effective way to treat cancer or reverse drug resistance[4–10]. Therefore, blocking the over-expression or activity of metabolism enzymes is an intellectual pursuit to develop anti-cancer drugs.

Valproic acid (VPA), a well-established drug in the long-term therapy of epilepsy, was first synthesized by Burton in 1882. Dr. Göttlicher discovered VPA as a Class I selective HDAC inhibitor[11]. Owing to its HDAC inhibiting capability, VPA is reported to play a critical role in anti-tumor activity in multiply cancer types[12]. Accumulating evidences support that VPA contributes to regulating a broad range of biological functions, including suppressing apoptosis, inhibiting cell proliferation, inducing autophagy and attenuating the epithelial-mesenchymal transition (EMT) in cancer cells[13–17]. However, the anti-tumor effects of VPA on the modulation of the Warburg effect in breast cancer remain under-investigated.

In this study, we discover that VPA suppresses breast cancer growth by inhibiting aerobic glycolysis through effects on PKM2 expression. Specifically, VPA regulates the Warburg effect via attenuating the level of ERK1/2 phosphorylation by targeting HDAC1. Taken together, targeting PKM2 with the HDAC1 inhibitor VPA in the Warburg effect may provide useful insights for the development of promising therapeutic strategies in breast cancer.

Materials and Methods

Cell Culture

MCF-7, MDA-MB-231 and HEK293 T cells were cultured in Dulbecco Modified Eagle Medium (high glucose) (DMEM, Gibco, ThermoFisher Scientific, Waltham, MA, USA) with 10% fetal bovine serum (FBS, HyClone, ThermoFisher Scientific), 100 U/mL penicillin and 100 μg/mL streptomycin at 37°C in a humidified atmosphere of 5% CO_2.

Cell Proliferation Assay

MCF-7, MDA-MB-231 or HEK293 T cells were plated in 6-well plates at a density of 5×10^4 cells per well for 24 h and treated with the absence or presence of VPA (Sigma-Aldrich, St. Louis, MO, USA) for 1, 2, 3 and 4 days. The cell numbers were counted at indicated days.

Colony Formation Assay

MCF-7 (600 cells/well) or MDA-MB-231 (6000 cells/well) cells were seeded in 6-well plates and cultured in the absence or presence of 2 mM or 4 mM VPA for 14 days. Cells were washed, fixed with methanol and stained with 1% methylene blue. The colony numbers were counted by using ImageJ software.

Western Blot

Western blot analysis was performed according to a standard procedure. Cells were lysed with lysis buffer [1.5 M NaCl, 1 M HEPES (pH 7.0), 0.1 M NaF, 0.1 M $Na_4P_2O_7$, 0.1 M Na_3VO_4, 1% NP40, protease inhibitor] on ice for 30 min and then centrifuged at 12000 r/min for 20 min at 4°C. Protein concentration was determined by a BCA protein assay kit (ThermoFisher Scientific). Equal amounts of protein were subjected to sodium dodecyl sulfate–polyacrylamide gel electrophoresis and transferred onto PVDF membranes (Merck Millipore, Darmstadt, Germany). Membranes were blocked with 5% non-fat milk in Tris-buffered saline-Tween (TBST) at room temperature for 1 h and then incubated overnight at 4°C with primary antibodies against HK2 (Cell Signaling Technology, CST, Danvers, MA, USA, #2867), GPI (Proteintech, Rosemont, IL, USA, #15171-1-AP), ALDOA (Proteintech, #11217-1-AP), GADPH (Proteintech, #60004-1-Ig), PGK1 (Abcam, Cambridge, MA, USA, #ab38007), PGAM1 (Proteintech, #16126-1-AP), ENO1 (Proteintech, #11204-1-AP), PKM2 (CST, #4053), LDHA (CST, #3582), ERK1/2 (CST, #4695), p-ERK1/2 (CST, #4370), β-actin (Proteintech, #60008-1-Ig). Membranes were washed with TBST and incubated with corresponding secondary antibodies HRP-linked anti-rabbit IgG (CST, #7074) or HRP-linked anti-mouse IgG (CST, #7076) for 1 h at room temperature. Immunoreactive bands were visualized using an enhanced chemiluminescence reaction kit (Merck Millipore) and were exposed on X-ray films (Kodak, Rochester, NY, USA). Quantification of Western blot by densitometry was assessed by using ImageJ software.

Cell Metabolism Determination

Extracellular acidification rate (ECAR) and oxygen consumption rate (OCR) were detected using the Seahorse XF^e 96 Extracellular Flux Analyzer (Agilent Technologies, Santa Clara, CA, USA) following the manufacturer's instructions. Briefly, MCF-7 or MDA-MB-231 cells were treated in the absence or presence of 2 mM or 4 mM VPA for 12 h and then 1×10^4 cells were plated into XF^e 96-well plates and pre-treated with or without VPA for 12 h. Cells were washed with Seahorse analysis media and incubated in a CO_2-free incubator at 37°C for 1 h. ECAR was measured using Glycolysis Stress Test Kit (Agilent). Glucose (10 mM), Oligomycin (1 μM) and 2-DG (100 mM) were injected into each well sequentially at the indicated time points. OCR was measured using Cell Mito Stress Test Kit (Agilent). Oligomycin (1 μM), FCCP (1 μM) and rotenone/antimycin A (0.5 μM) were injected into each well sequentially at the indicated time points. ECAR or OCR values were normalized to the protein concentration. Data were analyzed by Seahorse XF^e 96 Wave software.

Lactate Production Assay

MCF-7 cells were seeded in six-well plates and incubated at 37°C overnight. Fresh phenol red-free DMEM (Gibco) without FBS was added to the plate of 50%-confluent cells for 1 h. Aliquots of media from each well were assessed for the amount of lactate present. Cellular lactate production was determined by using the colorimetric-based lactate assay kit (Sigma-Aldrich) following the manufacturer's instructions and normalized to cell numbers.

Lentivirus Infection and Generation of Stable Cell Lines

shRNA plasmids targeting HDAC1, HDAC2 and HDAC3 were purchased from Transheep Biological Corporation (Shanghai, China). psPAX2, pMD2.G and pLKO-shRNA-expressing plasmids were co-transfected into HEK293 T cells using Polyethylenimine (PolyScience, Niles, Illinois, USA) following the manufacturer's protocol. 48 h after transfection, supernatant containing the lentivirus was harvested and mixed with 8 µg/mL polybrene then infected into MCF-7 cells. Cells were selected with 2 µg/mL puromycin and collected for Western blot analysis.

Real-Time Quantitative PCR

Total cellular RNA was isolated using TRIzol reagent according the manufacturer's instructions (Invitrogen, Carlsbad, CA, USA). RNA quality was assessed on NanoDrop ONE Microvolume UV-Vis Spectrophotometer (Thermo-Fisher Scientific) and checked using RNase free agarose gel electrophoresis. Total RNA was used as a template to reverse transcribe into cDNA using the PrimeScript RT reagent Kit with gDNA Eraser (TaKaRa, Japan), according to the manufacturer's protocol. Real-time quantitative PCR was performed in triplicates in a 20 µL reaction mixture containing 2× SYBR Green qPCR Master Mix (Bimake, Houston, TX, USA), 0.25 µM of each of the primers and 50 ng cDNA, using a CFX96 Connect Real-Time System instrument (BioRad, Hercules, CA, USA). Thermal cycling was initiated at 95°C for 10 min, followed by 40 cycles consisting of denaturation at 95°C for 15 s and combined annealing step at 60°C for 30 s, extension at 72°C for 30 s. A melting curve analysis was performed by gradually heating the samples from 60°C to 95°C with 0.5°C increment per second while the fluorescence was measured continuously. The relative expression level was calculated with the $2^{-\Delta\Delta CT}$ method. Data were normalized to reference gene (β-actin) expression and compared to the control group. The primers used for real-time qPCR analysis were as follows: *HDAC1* Forward: 5′-GGAAATCTATCGCCCTCACA-3′, Reverse: 5′-AACAGGCCATCGAATACTGG-3′; *HDAC2* Forward: 5′-ATGGCGTACAGTCAAGGAGG-3′, Reverse: 5′-TGC GGATTCTATGAGGCTTCA-3′; *HDAC3* Forward: 5′-GCA AGGCTTCACCAAGAGTCT-3′, Reverse: 5′-AGATGCG CCTGTGTAACGC-3′; β-*actin* Forward: 5′-ACGTGGA CATCCGCAAAG-3′, Reverse: 5′-GACTCGTCATACTC CTGCTTG-3′.

Xenograft Animal Model

All animal experiments were approved by the Xinhua Hospital Affiliated to Dalian University Animal Care and Use Committee and carried out in accordance with the regulations of the Service of Consumables and Veterinary Affairs-Division of Animal Protection (SCAV-EXPANIM). 10 female BALB/c nude mice were obtained from the Dalian medical university. 2×10^6 MDA-MB-231 cells were adjusted in 200 µL PBS and then inoculated into the subcutaneous part of the right breast of mice. Mice were randomized divided into two groups ($n = 5$). On day 6, The control group administered intraperitoneally injection of DMSO, while the VPA treatment group received intraperitoneal injection of VPA (500 mg/kg) every other day. The tumor growth of mice was monitored by the in vivo imaging system (IVIS) spectrum system (PerkinElmer, Waltham, MA, USA). After 30 days treatment initiation or when the tumor size reached 2 cm in diameter, mice were sacrificed.

Bioinformatics Analysis

Gene expression levels were analyzed by the public Gene Expression Omnibus datasets (GSE9574). The Human Protein Atlas dataset (https://www.proteinatlas.org) was used for immunohistochemical analysis. Correlations between PKM2 and HDAC1 protein expression in breast cancer were assessed by the Gene Expression Profiling Interactive Analysis (GEPIA) database (http://gepia.cancer-pku.cn/detail.php).

Statistical Analysis

All statistical analyses were performed with GraphPad Prism 6.0 (GraphPad Software, LA Jolla, CA, USA). The statistical differences were analyzed by unpaired, two-tailed Student's *t*-test or one-way ANOVA analysis. Data from three independent experiments are expressed as the mean ± standard deviation (SD). Results were considered statistically difference when $P < .05$.

Results

VPA Inhibits Oncogenesis in Breast Cancer Cells in Vitro

VPA was an effective HDAC inhibitor with a potent anti-tumor activity (Fig. 1A). In the present study, we focused on the anti-tumor activity of VPA in breast cancer. As a model system, we chose two different breast cancer subtypes MCF-7 and MDA-MB-231 cell lines. MCF-7 (estrogen-receptor positive) cell line is Luminal A type tumor which has been extensively studied the mechanism of estrogen-stimulated tumor growth. MDA-MB-231 (estrogen-receptor negative, progesterone receptor negative and HER2/neu oncogene negative) cell line which is
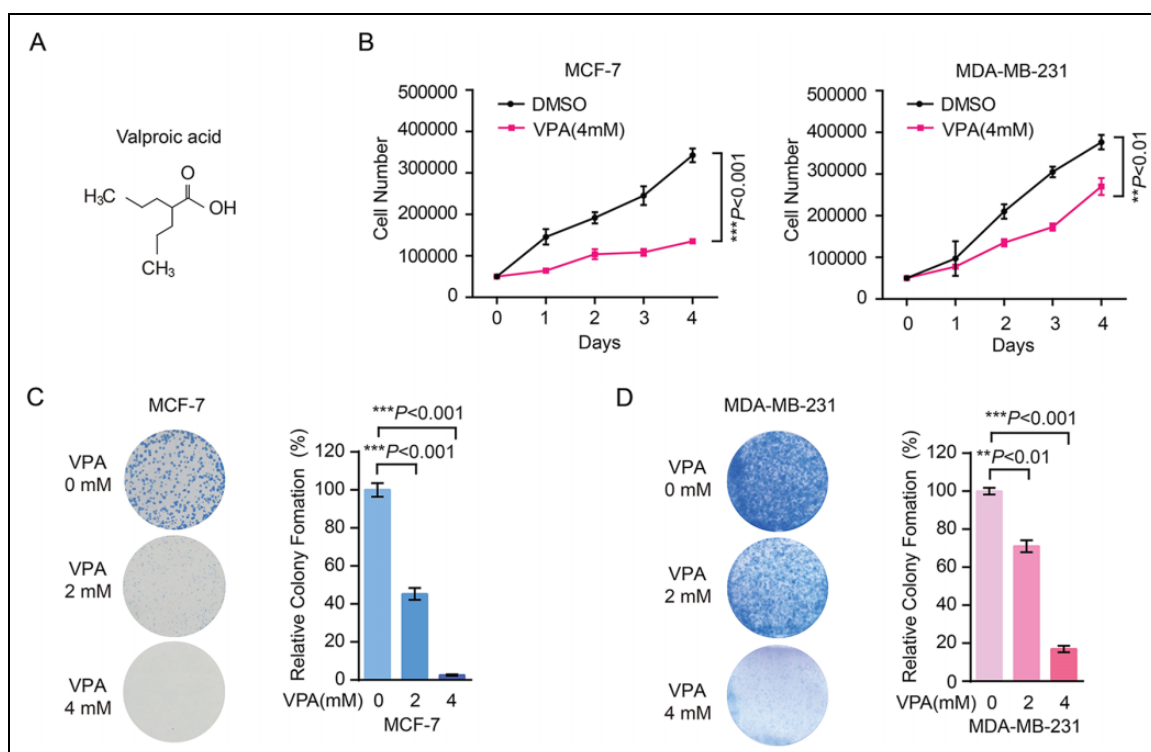
Figure 1. VPA inhibits oncogenesis in breast cancer cells in vitro. (A) Structure of VPA. (B) The cell proliferation of MCF-7 and MDA-MB-231 cells were decreased with 4 mM VPA treatment by cell number counting assay. Student's *t*-test was used for statistical analysis. Data represent mean $\pm$ SD from three biological replicates (**$P < .01$; ***$P < .001$). (C-D) The colony formation of MCF-7 (C) and MDA-MB-231 (D) cells were decreased with 2 mM or 4 mM VPA treatment. Representative images (left panel) and quantification (right panel) of colonies were shown. Statistical significances were calculated by Student's *t*-test. Data represent mean $\pm$ SD from three biological replicates (**$P < .01$; ***$P < .001$).
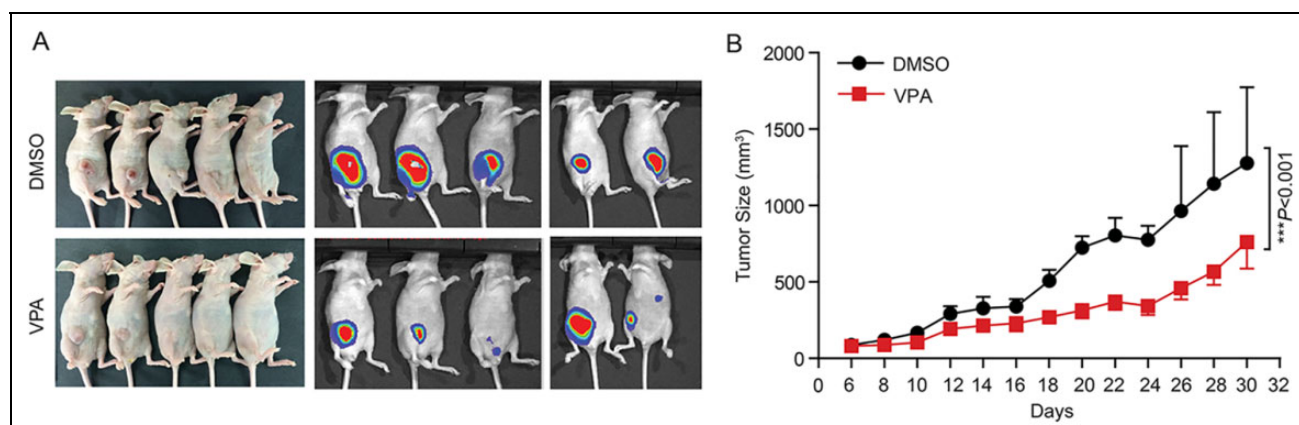

Figure 2. VPA inhibits breast cancer growth in vivo. (A) An IVIS imaging was performed to detect tumor growth in the MDA-MB-231 xenograft nude mice of DMSO group and VPA group. Representative bioluminescent images were shown ($n = 5$ biologically independent mice per group). (B) VPA reduced primary tumor growth significantly in the MDA-MB-231 xenograft model. Tumor size was measured every 2 days and growth curves were plotted. Statistical significances were calculated by Student's *t*-test. Data represent mean $\pm$ SD (***$P < .001$, $n = 5$ biologically independent mice per group).

invasive triple negative breast cancer (TNBC) type tumor and shows much more aggressive and malignant than MCF-7 cells, in consequence, often used in the study of tumor metastasis in breast cancer. We firstly found that VPA treatment remarkably suppressed the proliferation of MCF-7 and MDA-MB-231 cells (Fig. 1B). Additionally,

cell proliferation was inhibited in 293 T cells with VPA treatment as well (Supplemental Fig. S1). In the second, VPA treatment attenuated MCF-7 and MDA-MB-231 cells colony formation capability in a dose-dependent manner (Fig. 1C, D). Collectively, these data indicated that VPA inhibited oncogenesis in breast cancer cells in vitro.
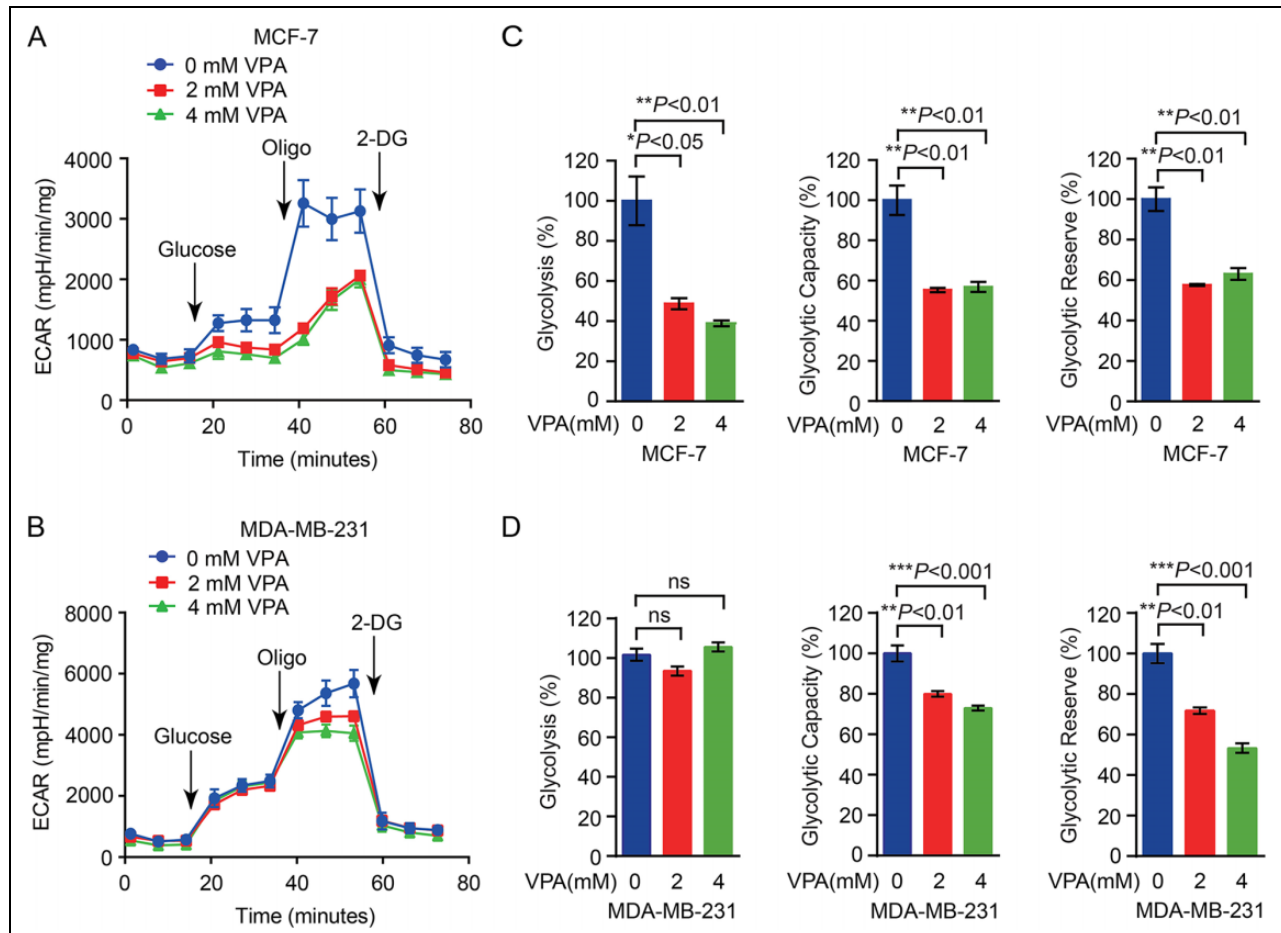
Figure 3. VPA attenuates the Warburg effect in breast cancer cells. (A-B) The glycolysis rate were decreased in MCF-7 (A) and MDA-MB-231 (B) cells with 2 mM or 4 mM VPA by ECAR (a proxy for the rate of glycolysis) analysis. Data represent mean $\pm$ SD from three biological replicates. (C-D) The parameters of glycolysis, glycolytic capacity and the glycolytic reserve were tested in MCF-7 (C) and MDA-MB-231 (D) cells with or without VPA treatment. Statistical significances were calculated by Student's t-test. Data represent mean $\pm$ SD from three biological replicates (*$P < .05$; **$P < .01$; ***$P < .001$; ns, not significant).

VPA Inhibits Breast Cancer Growth in Vivo

Based on the in vitro results, we subcutaneously injected MDA-MB-231 cells into nude mice and tumors were imaged after 30 days implantation and dosing. In contrast, the mice in VPA group displayed weaker bioluminescent signal in tumors and the mean tumor size was significantly smaller compared with the DMSO group (Fig. 2A, B). Of note, VPA treatment dramatically retarded tumor growth in vivo. As a consequence, these results strongly illustrated that VPA impaired tumorigenicity of breast cancer cells.

VPA Attenuates the Warburg Effect in Breast Cancer Cells

Next, we elucidated the mechanism of VPA inhibiting breast cancer growth from the Warburg effect angle, which played an essential role in regulating cancer cell growth. MCF-7 and MDA-MB-231 cells treated with VPA displayed reduced extracellular acidification rate (ECAR), which was a crucial indicator of aerobic glycolysis (Fig. 3A, B). Furthermore, VPA treatment correlated notably with a decrease of the glycolytic capacity and the glycolytic reserve in MCF-7 and MDA-MB-231 cells, key parameters of glycolytic flux (Fig. 3C, D). Nevertheless, there is still a little difference between MCF-7 and MDA-MB-231 cells about the sensitive of VPA treatment, that may be a predominant result of the different genetic backgrounds between these two cell lines. Subsequently, treatment of MCF-7 cells with VPA led to reduced lactate production (Supplemental Fig. S2A). Additionally, exposure to VPA decreased oxygen consumption rate (OCR) in MCF-7 cells, which stood for mitochondrial respiration (Supplemental Fig. S2B, C). These results suggested that VPA treatment attenuated aerobic glycolysis and oxidative phosphorylation in breast cancer cells.
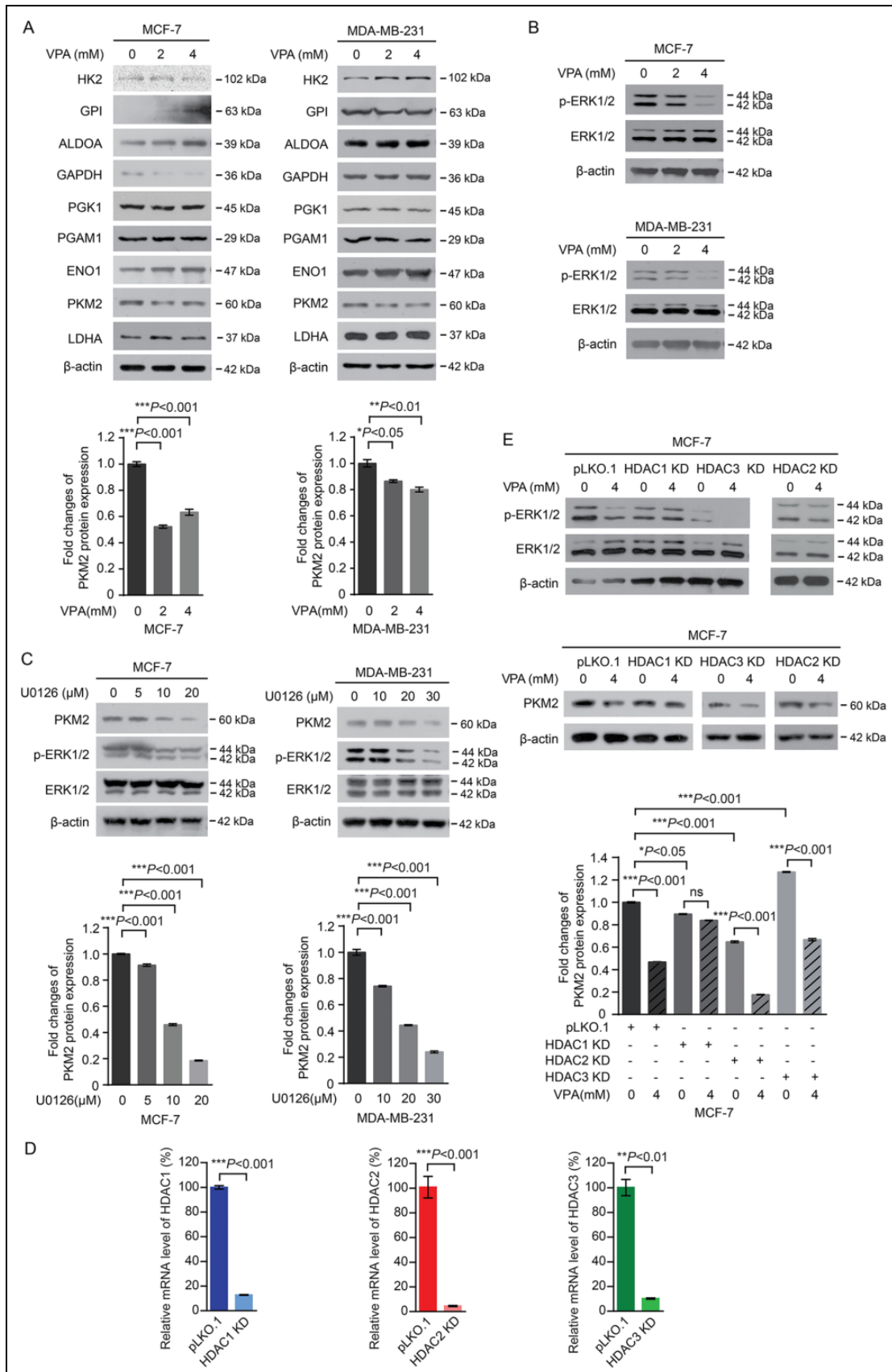
Figure 4. VPA affects the Warburg effect through down-regulated PKM2 expression via inhibiting ERK1/2 mediated by HDAC1. (A) The expression of glycolytic enzymes in MCF-7 and MDA-MB-231 cells untreated or treated with 2 mM or 4 mM VPA were determined by

VPA Affects the Warburg Effect through Down-Regulated PKM2 Expression via Inhibiting ERK1/2 Mediated by HDAC1

To gain further insights into the mechanism underlying VPA in regulating aerobic glycolysis, we determined the expression of a number of key enzymes in the glycolysis pathway. VPA treatment decreased PKM2 protein expression in MCF-7 and MDA-MB-231 cells (Fig. 4A), indicating that VPA repressed glycolysis in breast cancer cells by reducing the expression of PKM2. Moreover, the levels of extracellular signal-regulated kinase (ERK1/2) phosphorylation were significantly decreased when MCF-7 and MDA-MB-231 cells were treated with VPA (Fig. 4B). Importantly, we also observed that PKM2 expression was reduced by ERK1/2 inhibitor U0126 treatment in concentration-dependent manners in MCF-7 and MDA-MB-231 cells (Fig. 4C). Similar results were observed in HEK293 T cells (Supplemental Fig. S3). These results were in line with the research showing that ERK1/2-dependent nuclear PKM2 promoted the Warburg effect in brain tumor[18]. It has been reported that VPA mainly targets to HDAC1, HDAC2, and HDAC3. To better understand the molecular mechanism of VPA in regulating PKM2 expression mediated by ERK1/2 activity, we generated HDAC1, HDAC2 and HDAC3 stable knockdown cells in MCF-7 cells. The knockdown efficiencies of HDAC1, HDAC2 and HDAC3 were confirmed by RT-qPCR (Fig. 4D). We determined the ERK1/2 phosphorylation levels and PKM2 expression in HDAC1, HDAC2 and HDAC3 knockdown MCF-7 cells with VPA treated. Principally, HDAC1 knockdown in MCF-7 cells blocked the effect of VPA on ERK1/2 phosphorylation while decreasing PKM2 expression (Fig. 4E). Collectively, these results explained that VPA regulated PKM2 expression triggering Warburg effect through ERK1/2 signaling pathway targeting HDAC1.

PKM2 and HDAC1 Expression are Elevated in Breast Cancer

We then sought to further decipher the role of PKM2 in breast cancer progression. By interrogating the Gene Expression Omnibus (GEO) profiles (GSE9574), we revealed remarkably higher expression of PKM2 in cancer tissues compared with the normal tissues (Fig. 5A). Besides, HDAC1 expression was higher in cancer tissues than in non-tumor tissues but not HDAC2 and HDAC3 (Fig. 5B–D). To gain additional clinical insights, immunohistochemical analyses were assessed by the Human Protein Atlas dataset. Consistently, higher PKM2 and HDAC1 expression levels were also observed in breast cancer tissues (Fig. 5E). In addition, higher PKM2 protein expression was positively correlated with HDAC1 expression in breast cancer from GEPIA database (Fig. 5F). Together, these results demonstrated that targeting HDAC1 by VPA impaired Warburg effect via down-regulating PKM2 expression mediated by ERK1/2 inactivation, thus inhibiting breast cancer cell growth (Fig. 5G).

Discussion

The strategy of "rediscovery of old drugs for new uses," which possesses merits of reducing the cost and shortening the time of drug development and preclinical research, has been widely concerned over the past decade and applied in systems pharmacology and clinical practice. A case in point is VPA, which is used for epilepsy therapy, while it recently has been validated to have potent efficacies against tumor. Cancer metabolism has gained increasing attention in recent years. The Warburg effect enhances glucose uptake and produces ATP quickly through aerobic glycolysis to meet the energy and biosynthesis demands for rapid cancer cell growth. Emerging studies have focused on targeting metabolism enzymes in cancer treatment, which seems appealing at first glance[9,19]. As a glycolytic enzyme, pyruvate kinase (PK) is a critical rate-limiting mediator of the Warburg effect that catalyzes the irreversible transfer of phosphate from phosphoenolpyruvate (PEP) to adenosine diphosphate (ADP) and produces pyruvate and ATP. Among four isoforms of PK, M2 isoform (PKM2) is exclusively expressed in most tumor cells, identifying PKM2 as an exciting avenue for cancer therapy[20,21]. In this study, we demonstrated that PKM2 was generally up-regulated in breast cancer according to the clinical bioinformatics data. VPA treatment could block cell proliferation and tumor growth in breast cancer

Figure 4. (Continued). Western blot assay (top panel). Densitometry analysis was performed to assess the PKM2 expression (normalized to β-actin expression) and presented as fold changes over untreated cells (bottom panel). Statistical significances were calculated by Student's *t*-test. Data represent mean ± SD from three biological replicates (*P < .05; **P < .01; ***P < .001). (B) Western blot assay showed the levels of p-ERK1/2 were decreased in MCF-7 and MDA-MB-231 cells treated with 2 mM or 4 mM VPA. (C) Western blot assay showed the expression of PKM2 was down-regulated in MCF-7 and MDA-MB-231 cells in the presence of U0126 (top panel). Densitometry analysis was performed to assess the PKM2 expression (normalized to β-actin expression) and presented as fold changes over untreated cells (bottom panel). Statistical significances were calculated by Student's *t*-test. Data represent mean ± SD from three biological replicates (***P < .001). (D) The knockdown efficiencies of HDAC1, HDAC2, and HDAC3 in HDAC1, HDAC2, and HDAC3 knockdown MCF-7 cells were determined by Real-time qPCR. β-actin was used as control. Statistical significances were calculated by Student's *t*-test. Data represent mean ± SD from three biological replicate (**P < .01; ***P < .001). (E) The levels of p-ERK1/2 and expression of PKM2 in HDAC1, HDAC2, and HDAC3 knockdown MCF-7 cells with or without VPA treatment were determined by Western blot assay (top panel). Densitometry analysis was performed to assess the PKM2 expression (normalized to β-actin expression) and presented as fold changes over untreated cells (bottom panel). Statistical significances were calculated by one-way ANOVA analysis. Data represent mean ± SD from three biological replicates (*P < .05; ***P < .001; ns, not significant).
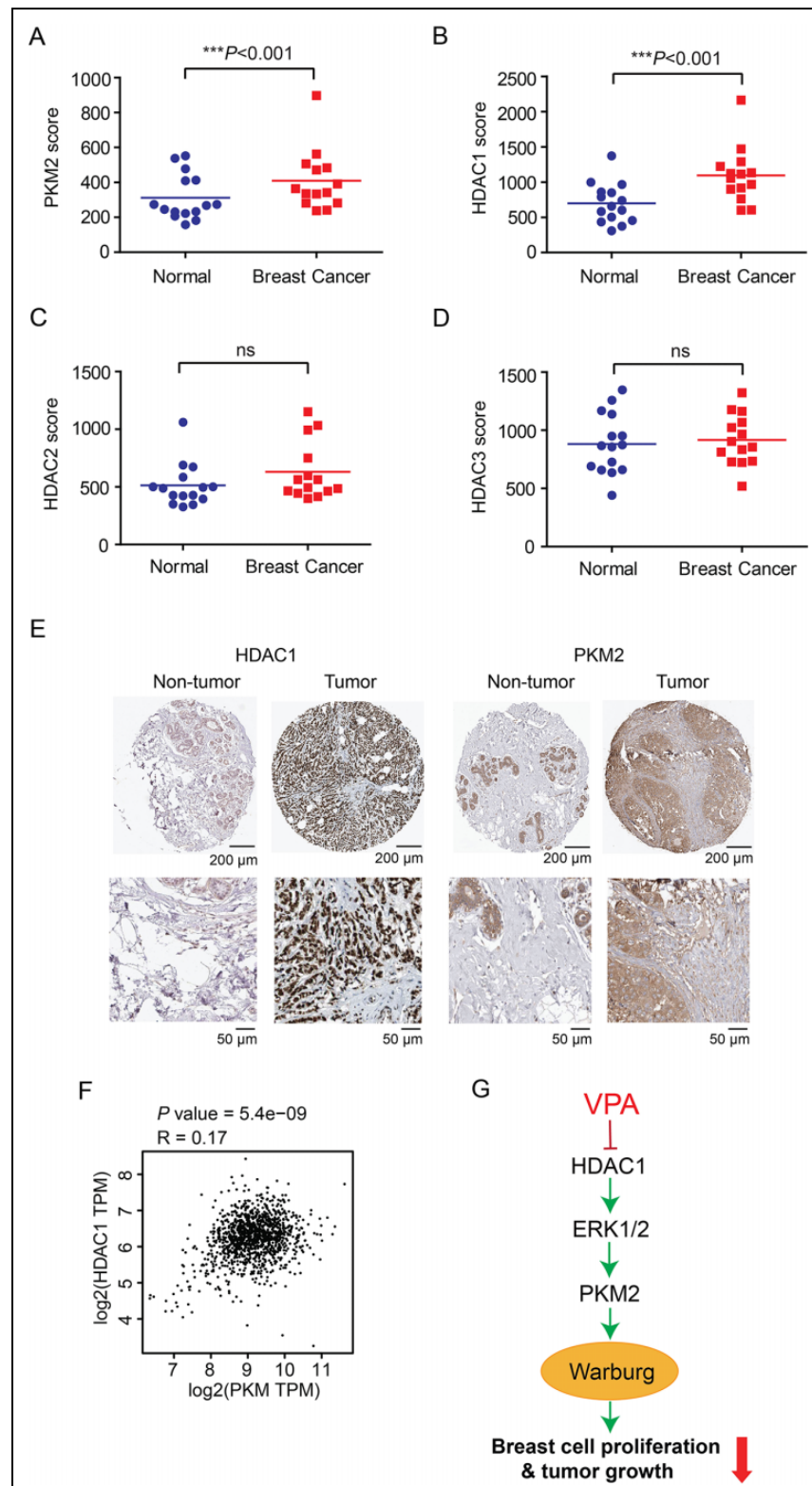
Figure 5. PKM2 and HDAC1 expression are elevated in breast cancer. (A-D) Gene expression levels of PKM2 (A), HDAC1 (B), HDAC2 (C) and HDAC3 (D) in breast cancer tissues and normal tissues, calculated from GEO profiles (GSE9574, normal number = 15, breast cancer number = 14). Student's *t*-test was used for statistical analysis (***P < .001; ns, not significant). (E) Representative IHC images showed the increase of PKM2 and HDAC1 expression in breast tumor tissues compared to normal breast tissues from the Human Protein Atlas datasets (scale bar: original magnification 200 μm, inset magnification 50 μm). (F) Scatterplot showing the positive correlation between PKM2 and HDAC1 expression in breast cancer from GEPIA database. (G) The schematic model shows that the role and mechanism of VPA in regulating breast cancer growth.

cell lines. Importantly, VPA suppressed the aerobic glyco-
lysis and tumor progression in breast cancer by decreasing
the expression of PKM2. It is particularly noteworthy that
the low enzymatic activity of PKM2 is required for the War-
burg effect[22]. Further investigation about PKM2 enzymatic
activity involved in the regulation of VPA on Warburg effect
is needed to refine our understanding. Overall, our study
indicates that VPA is an anti-proliferative agent for Warburg
effect. Notably, it was recently reported that the inhibition of
glycolysis decreased the cancer stem cells population in
tumor niche and thereby reduced tumor resistance to thera-
pies[23]. Taken together, targeting Warburg effect by VPA
seems to be an effective therapeutic strategy against breast
cancer which is highly desirable.

Histone deacetylation is a common epigenetic modifica-
tion and acts a pivotal part in gene expression and signal
transduction, which recently has been exploited as prime
anti-cancer drug target. VPA is a HDAC inhibitor, but the
signaling pathway by which VPA modulates has not been
elucidated, especially in cancer metabolism. ERK1/2 signal-
ing pathway is strongly implicated in cancer. ERK1/2 activa-
tion catalyzes the phosphorylation of downstream
transcription factors and regulatory molecules rapidly in
response to stimulations, which is vital for various cellular
activities and physiological processes such as cell cycle pro-
gression, cell survival, proliferation, differentiation and meta-
bolism[24]. Here, we discovered that the expression of HDAC1
was elevated in breast tumor tissues and the higher PKM2
expression was positively related to the HDAC1 expression
in breast cancer. Moreover, the reduction in HDAC1 expres-
sion by VPA may inactivate the ERK1/2 signaling pathway
and combine with decreased PKM2 expression, resulting in
suppressing the Warburg effect (Fig. 5G). It helps to under-
stand the molecular mechanism by which signaling pathway
VPA regulates in the Warburg effect and also gives rise to the
role that VPA plays in breast cancer therapy.

Conclusion

Collectively, our data indicated that HDAC1 inhibitor VPA
could reprogram the Warburg effect and suppress cancer
growth through the negative regulation of PKM2 expression
mediated by ERK1/2 signaling pathway.

It is conceivable that VPA might be a therapeutically
effective drug targeting glycolysis metabolism against breast
cancer, which is expected to have important therapeutic
implications.

Ethical Approval

Ethical approval was obtained for all experimental procedures from
the Xinhua Hospital Affiliated to Dalian University Animal Care
and Use Committee, Liaoning, China.

Statement of Human and Animal Rights

All procedures in this study were conducted in accordance with the
Xinhua Hospital Affiliated to Dalian University Animal Care and

Use Committee, Liaoning, China and carried out in accordance
with the regulations of the Service of Consumables and Veterinary
Affairs-Division of Animal Protection (SCAV-EXPANIM).

Statement of Informed Consent

There are no human subjects in this article and informed consent is
not applicable.

Declaration of Conflicting Interests

The author(s) declare no potential conflicts of interest with respect
to the research, authorship, and/or publication of this article.

ORCID iD

Zhen Li https://orcid.org/0000-0003-0436-8999

Supplemental Material

Supplemental material for this article is available online.

References

1. Sung H, Ferlay J, Siegel RL, Laversanne M, Soerjomataram I,
   Jemal A, Bray F. Global cancer statistics 2020: GLOBOCAN
   estimates of incidence and mortality worldwide for 36 cancers
   in 185 countries. CA Cancer J Clin. 2021;71(3):209–249.
2. Chaffer CL, Weinberg RA. A perspective on cancer cell metas-
   tasis. Science. 2011;331(6024):1559–1564.
3. Cairns RA, Harris IS, Mak TW. Regulation of cancer cell
   metabolism. Nat Rev Cancer. 2011;11(2):85–95.
4. Fan J, Shan C, Kang HB, Elf S, Xie J, Tucker M, Gu TL,
   Aguiar M, Lonning S, Chen H, Mohammadi M, et al. Tyr
   phosphorylation of PDP1 toggles recruitment between ACAT1
   and SIRT3 to regulate the pyruvate dehydrogenase complex.
   Mol Cell. 2014;53(4):534–548.
5. Liu H, Liu Y, Zhang JT. A new mechanism of drug resistance
   in breast cancer cells: fatty acid synthase overexpression-
   mediated palmitate overproduction. Mol Cancer Ther. 2008;
   7(2):263–270.
6. Wang JB, Erickson JW, Fuji R, Ramachandran S, Gao P, Dina-
   vahi R, Wilson KF, Ambrosio AL, Dias SM, Dang CV, Cer-
   ione RA. Targeting mitochondrial glutaminase activity inhibits
   oncogenic transformation. Cancer Cell. 2010;18(3):207–219.

7. Zhao Y, Butler EB, Tan M. Targeting cellular metabolism to improve cancer therapeutics. Cell Death Dis. 2013;4:e532.

8. Zhao Y, Liu H, Liu Z, Ding Y, Ledoux SP, Wilson GL, Voellmy R, Lin Y, Lin W, Nahta R, Liu B, et al. Overcoming trastuzumab resistance in breast cancer by targeting dysregulated glucose metabolism. Cancer Res. 2011;71(13): 4585–4597.

9. Zheng W, Feng Q, Liu J, Guo Y, Gao L, Li R, Xu M, Yan G, Yin Z, Zhang S, Liu S, et al. Inhibition of 6-phosphogluconate dehydrogenase reverses cisplatin resistance in ovarian and lung cancer. Front Pharmacol. 2017;8:421.

10. Zhou M, Zhao Y, Ding Y, Liu H, Liu Z, Fodstad O, Riker AI, Kamarajugadda S, Lu J, Owen LB, Ledoux SP, et al. Warburg effect in chemosensitivity: targeting lactate dehydrogenase-A re-sensitizes taxol-resistant cancer cells to taxol. Mol Cancer. 2010;9:33.

11. Gottlicher M, Minucci S, Zhu P, Kramer OH, Schimpf A, Giavara S, Sleeman JP, Lo Coco F, Nervi C, Pelicci PG, Heinzel T. Valproic acid defines a novel class of HDAC inhibitors inducing differentiation of transformed cells. EMBO J 2001; 20(24):6969–6978.

12. Botrugno OA, Robert T, Vanoli F, Foiani M, Minucci S. Molecular pathways: old drugs define new pathways: non-histone acetylation at the crossroads of the DNA damage response and autophagy. Clin Cancer Res. 2012;18(9):2436–2442.

13. Fortunati N, Bertino S, Costantino L, Bosco O, Vercellinatto I, Catalano MG, Boccuzzi G. Valproic acid is a selective antiproliferative agent in estrogen-sensitive breast cancer cells. Cancer Lett. 2008;259(2):156–164.

14. Gao D, Xia Q, Lv J, Zhang H. Chronic administration of valproic acid inhibits PC3 cell growth by suppressing tumor angiogenesis in vivo. Int J Urol. 2007;14(9):838–845.

15. Tassara M, Dohner K, Brossart P, Held G, Gotze K, Horst HA, Ringhoffer M, Kohne CH, Kremers S, Raghavachar A, Wulf G, et al. Valproic acid in combination with all-trans retinoic acid and intensive therapy for acute myeloid leukemia in older patients. Blood. 2014;123(26):4027–4036.

16. Xia Q, Zheng Y, Jiang W, Huang Z, Wang M, Rodriguez R, Jin X. Valproic acid induces autophagy by suppressing the Akt/mTOR pathway in human prostate cancer cells. Oncol Lett. 2016;12(3):1826–1832.

17. Lan X, Lu G, Yuan C, Mao S, Jiang W, Chen Y, Jin X, Xia Q. Valproic acid (VPA) inhibits the epithelial-mesenchymal transition in prostate carcinoma via the dual suppression of SMAD4. J Cancer Res Clin Oncol. 2016;142(1):177–185.

18. Yang W, Zheng Y, Xia Y, Ji H, Chen X, Guo F, Lyssiotis CA, Aldape K, Cantley LC, Lu Z. ERK1/2-dependent phosphorylation and nuclear translocation of PKM2 promotes the Warburg effect. Nat Cell Biol. 2012;14(12):1295–1304.

19. Zhong XY, Yuan XM, Xu YY, Yin M, Yan WW, Zou SW, Wei LM, Lu HJ, Wang YP, Lei QY. CARM1 Methylates GAPDH to Regulate Glucose Metabolism and Is Suppressed in Liver Cancer. Cell Rep. 2018;24(12):3207–3223.

20. Wong N, Ojo D, Yan J, Tang D. PKM2 contributes to cancer metabolism. Cancer Lett. 2015;356(2 Pt A):184–191.

21. Dayton TL, Jacks T, Vander Heiden MG. PKM2, cancer metabolism, and the road ahead. EMBO Rep. 2016;17(12):1721–1730.

22. Christofk HR, Heiden MGV, Harris MH, Ramanathan A, Gerszten RE, Wei R, Fleming MD, Schreiber SL, Cantley LCJN. The M2 splice isoform of pyruvate kinase is important for cancer metabolism and tumour growth. Nature. 2008; 452(7184):230–233.

23. Pouyafar A, Heydarabad MZ, Abdolalizadeh J, Zade JA, Rahbarghazi R, Talebi M. Modulation of lipolysis and glycolysis pathways in cancer stem cells changed multipotentiality and differentiation capacity toward endothelial lineage. Cell Biosci. 2019;9:30.

24. Roskoski R Jr. ERK1/2 MAP kinases: structure, function, and regulation. Pharmacol Res. 2012;66(2):105–143.